Separation Science and Technology
Publication details, including instructions for authors and subscription information:
http://www.informaworld.com/smpp/title~content=t713708471

Chromatographic Separations by Pillared Clay

M. S. A. Baksh[a]; R. T. Yang[a]
[a] Department Of Chemical Engineering, State University Of New York At Buffalo, Buffalo, New York

To cite this Article Baksh, M. S. A. and Yang, R. T.(1991) 'Chromatographic Separations by Pillared Clay', Separation Science and Technology, 26: 10, 1377 — 1394
To link to this Article: DOI: 10.1080/01496399108050538
URL: http://dx.doi.org/10.1080/01496399108050538

SEPARATION SCIENCE AND TECHNOLOGY, **26**(10 & 11), pp. 1377–1394, 1991

Chromatographic Separations by Pillared Clay

M. S. A. BAKSH and R. T. YANG
DEPARTMENT OF CHEMICAL ENGINEERING
STATE UNIVERSITY OF NEW YORK AT BUFFALO
BUFFALO, NEW YORK, 14260

Abstract

Pillared interlayered clays have been prepared from Bentonite clay by reacting with zirconyl chloride solution. These new adsorbents have been characterized by adsorption isotherms, x-ray diffraction, and the diffusivities of probe molecules into these adsorbents. Using the sorbent, the separations of air, N_2/CH_4, C_6H_6/C_6H_{14}, CH_4/CO_2, and the C_8 aromatic isomers have been accomplished by equilibrium and/or kinetic separations via chromatography.

INTRODUCTION

Pillared interlayered clays (PILC) are two-dimensional, zeolite-like materials prepared by ion exchanging the interlayer cations of the clay with hydroxy-oligomeric metal cations. Upon heating, dehydration and dehydroxylation of the hydroxy metal cations occur, forming stable metal oxide clusters or pillars that separate the clay layers and create interlayer spaces of molecular dimensions. Since the first successful syntheses of PILC in the late 1970s (*1–6*), much interest has been directed toward PILC (*7–9*). In addition, different types of pillared clays were synthesized by inserting various metal oxides or salts that form polynuclear species upon hydrolysis (*10*) into layered clays (*8*, *11–13*).

Pillared clays have been used almost exclusively for catalytic applications (*7–9*), and only very limited measurements of the adsorption isotherms and diffusivities in pillared clays exist in the literature (*14–18*). Also, possible applications of pillared clays as new adsorbents in separation processes remain unexplored.

In this study, pillared clays were synthesized using hydroxy zirconium oligomeric cations, characterized, and were successfully used as the sorbents for separation. Since the separations of air (*19–21*), mixtures of CO_2/CH_4 (*22*), and N_2/CH_4 (*23*) are of commercial importance, these

mixtures were selected as the adsorbates, and Zr-PILC as the adsorbent in the gas chromatography experiments. In addition, the separation of C_8-aromatic isomers (ethylbenzene, *o*-xylene, *m*-xylene, and *p*-xylene) is also a challenging problem due to the low relative volatilities of the mixture components; therefore, we have included this mixture in our investigation. Also, the separation of the C_8-aromatic isomers is worthwhile since each component of the mixture serves as a feedstock for different chemicals production, e.g., *p*-xylene in the production of terephthalic acid, *o*-xylene to produce phthalic anhydride, ethylbenzene to form styrene, and *m*-xylene to produce isophthalic acid. Some of the prominent commercial processes for the separation of *p*-xylene are the UOP parex process (*24*), the Aromax process (*25*), and the Asahi process (*26*). Other processes used for the separation of the C_8-aromatic isomers have been reviewed (*27*). The separation of other mixtures using Zr-PILC are also possible, e.g., hexane diffuses much faster than benzene in Zr-PILC, and we have shown in this work that it is possible to separate a mixture of these components using a kinetic mode of operation.

In our earlier study the micropore size distributions of the pillared clays used in the present work were determined by molecular probing and adsorption data along with a theoretical framework for calculations (*28*). It was demonstrated that the interpillar spacings were substantially smaller than the interlayer spacings, and that the tailoring of the interpillar spacings was possible (*28*). Limited results on equilibrium isotherms and chromatographic separations were also given. In this paper we report further results on chromatographic separations and equilibrium isotherms as well as a detailed description of the synthesis procedure.

EXPERIMENTAL

Zr-PILC Synthesis

The starting clay was a purified grade of Bentonite Powder (Fisher Scientific P/N, Lot 880423). No attempt was made to remove any impurities that might be present in the material. Zirconium was supplied by Fisher Scientific as solid zirconyl chloride ($ZrOCl_2 \cdot 8H_2O$). The adsorbates used included xylenes, benzene, 1,3,5-trimethylbenzene, and hexane—all of ACS grades purchased from Fisher Scientific. All of the gases were supplied by Cryogenic Supply (Union Carbide Corp.), with a minimum purity of 99.9%.

The first step in PILC synthesis is the preparation and aging of the pillaring solutions. The oligomeric solutions were aged at 25°C for 10 days, and their pH values were maintained at 1.3. The aqueous chemistry of the oligomeric solution is complex and beyond the scope of this paper. The

tetramer $Zr_4(OH)_{14}(H_2O)_{10}^{2+}$ is believed to undergo hydrolysis, polymerization, and complex formation with anions. A more complete discussion of the hydrolysis of Zr cations is contained in the text of Baes and Mesmer (*10*). The slurry was prepared by dispersing the clay in deionized distilled water by vigorously stirring with the aid of a magnetic stirrer (the pH of this suspension was about 9.10 [1.0 g clay + 100 mL H_2O]), then the oligomeric solution (normally 25 cm^3) was added dropwise to the 1.0-g clay suspension while vigorous stirring was maintained. The addition of the solution took about 20 min. The slow addition of the oligomeric solution helps in the formation of uniform pillared clays. The pH of the resulting slurry was checked and adjusted to the desired value using 0.1 *M* HCl or 0.1 *M* NaOH. The adjusted pH of the slurries used in this study were in the range 1.4–8.35. This mixture is referred to as the *slurry* hereafter.

Once the slurries were prepared, the flasks were capped and placed inside a temperature-controlled waterbath shaker. The waterbath shaker kept the clay in suspension during the incubation period. Occasionally, some of the clay particles settled to the bottom of the flask. These flasks were removed and swirled vigorously by hand. After redispersion of the clay, the flasks were then returned to the waterbath shaker. The samples were kept in the waterbath for 3 days at a temperature of 50°C and then removed. The next step in the synthesis was vacuum filtration.

The vacuum filtration unit consisted of an aspirator attached to running water to create a vacuum, side-arm conical flask, ceramic perforated filter housing, rubber stopper, and Whatman filter paper. An appropriate vacuum level was controlled by adjusting the water flow rate. Excessive vacuum caused immediate plugging of the filter paper. Conversely, too low of a vacuum resulted in an excessively long filtration time. After gaining some experience with the filtration system, the separation of the clay from the suspension was optimized (less than 25 min per sample). The clay slurry was poured into the ceramic perforated housing lined with Whatman filter paper. The residue on the filter paper was washed several times with deionized distilled water to remove all chloride ions. The presence of chloride ions in the filtrate was determined using aqueous $AgNO_3$ to form AgCl precipitate. When precipitate no longer formed, washing was stopped. Normally, about 500 cm^3 of deionized distilled water was required per 1.0 g of clay slurry. After filtration, the filter paper containing the residue was removed from the filter housing and placed on a tray for air drying. Separation of the filter paper from the clay was easily accomplished once the clay had dried. The clay was transferred to a quartz dish for oven drying and calcination at elevated temperatures.

A three-step heating process was used. The muffle furnace temperature was raised to 100°C and kept at that temperature for 4 h. The temperature

was raised to 200°C, and the samples were soaked for 10 h. Finally, the samples were calcined at 350°C for 24 h. After calcination, the muffle furnace was turned off, the samples were removed and ground to 80–100 mesh size using a mortar and pestle, and then stored in capped vials. Samples Zr(1-6)E6 were prepared by varying the pH of the slurries in the 1.4–8.35 range and using 0.1 *M* $ZrOCl_2$ solution.

The adsorbent used in the gas chromatograph experiments was the pillared clay possessing the highest surface area (Zr2E6). The pillared clay was sieved to 80–100 mesh size before being packed into 1/4 and 1/8 in. outer diameters stainless steel tubes of desired lengths. Once the tubes were packed and capped at both ends, they were then configured to fit into a Gow-Mac Series 550 Gas Chromatograph equipped with a thermal conductivity detector. The adsorbent was regenerated at 150°C prior to the separation experiments by using helium as the purging gas. In all of the experiments, the adsorbates were introduced at the inlet of the column as an impulse, and helium was used as the carrier gas.

Isotherms and Diffusivity Measurements

Equilibrium isotherms and uptake rate curves were measured using a microbalance (Mettler TA2000C Thermoanalyzer) which was connected to a gas flow system. This apparatus consisted of supply gases that were attached to zeolite driers, wash bottles containing liquid adsorbates, pure gases, TGA microbalance, controllers, and a chart recorder. The driers were packed with 5A zeolites, and connected to different gases (He, CH_4, N_2, CO_2, and O_2). The flow system and the experimental procedures were similar to that described elsewhere (*29*). Gas mixture composition was determined by using a Gow-Mac 550 gas chromatograph equipped with a thermal conductivity detector. In some analyses of mixture compositions, a flame ionization detector was preferred and used for organic mixtures. Liquid adsorbates were placed in gas wash bottles (bubblers), and helium gas was flowed through the liquid to generate vapors. Samples of about 50 mg were used in the adsorption and diffusivity measurements.

Zr-PILC Characterization

A Quantasorb Surface Area Analyzer (Quantachrome Corporation) was used for the BET surface area determination. Prior to surface area measurements, each sample was outgassed at 200°C for 15 h. The N_2 desorption isotherms at 77 K were used in the surface area analysis. In addition, this instrument was also used for measuring N_2 adsorption isotherms at 77 K.

A Nicolet/Stoe powder diffractometer with position sensitive detector (PSD) was used in the XRD experiments. The powder sample (80–100

mesh) was sandwiched between Mylar films and mounted on a disk, which was then connected to a rotating spindle. The disk containing the sample intercepted the x-ray beam (CuK_α radiation), and the transmitted beam then entered the PSD detector through a side window.

The chemical compositions of the bentonite and Zr-pillared clays were determined by using a Thermo Jarrel Ash 61 Inductively Coupled Argon Plasma Atomic Emission Spectrometer (ICAP-AES). A description of this method is given by Lichte et al. (*30*). The sample solution was delivered to the nebulizer at 0.8 cm^3/min, and was carried to the plasma by the carrier gas (argon). All elemental concentrations except zirconium were determined by the polychromator, while zirconium was measured by the monochromator attachment using a wavelength setting of 339.1 nm. The instrument was calibrated using elemental standard solutions.

Clay samples were prepared for ICAP-AES analysis by using a fusion dissolution technique. Each sample of 100 mg was combined thoroughly with 0.6 g of 1:2 lithium metaborate–lithium tetraborate fluxing mixture. This dry powder mixture was then placed in a graphite crucible and fused in an oven at 1000°C for approximately 45 min. After cooling, the fused glass bead was added to a hot aqueous solution (250 cm^3) containing 10 cm^3 of a 1:1 HNO_3. The glass bead was completely dissolved in several hours as the solution was vigorously stirred while cooling to room temperature. The solution was filtered to remove graphite fibers prior to ICAP-AES analysis.

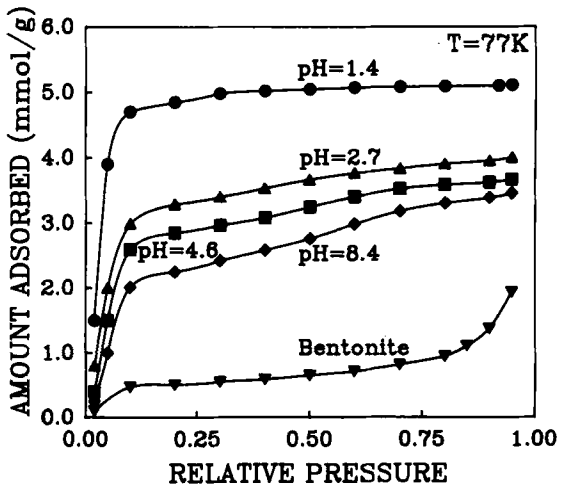

FIG. 1. Equilibrium isotherms on Zr-pillared clays prepared from slurries having different pH values. The unpillared clay (bentonite) is included for comparison.

RESULTS AND DISCUSSIONS

Adsorption Isotherms

The adsorption isotherms of nitrogen, oxygen, methane, carbon dioxide, hexane, benzene, ethylbenzene, and xylenes (*o*-xylene, *m*-xylene, and *p*-xylene) are displayed in Figs. 1–5. The nitrogen adsorption isotherms at 77 K (Fig. 1) show declining adsorption capacities with increasing pH of the slurries. Also, the isotherm for the lowest slurry pH (1.4), showing the highest N_2 adsorption capacity, corresponds to the Zr-pillared clay with the highest degree of microporosity. Thus, as the pH of the slurry increases, the corresponding pillared clay becomes less microporous; consequently, larger pores are formed (*28*), and the isotherms become less steep in the low relative pressure region.

The isotherms of O_2 and N_2 at 298 K on Zr-pillared clay (Zr2E6), are shown in Fig. 2. The isotherms show that the adsorption capacities reach limiting values at a pressure of about 1 atm due to the limiting pore volume in the pillared clay. The isotherms of nitrogen, methane, and carbon dioxide displayed in Fig. 3 indicate small equilibrium selectivities of CH_4/N_2 and CH_4/CO_2 on Zr-pillared clay (Zr2E6). The isotherms of *n*-hexane and benzene are displayed in Fig. 4. The equilibrium selectivity for *n*-hexane/benzene is not high enough for separation. However, as will be shown later, the diffusivities are high enough to effect a kinetic separation.

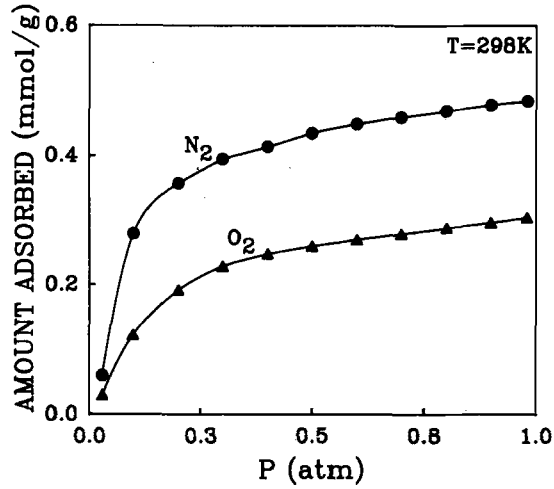

FIG. 2. Equilibrium isotherms of N_2 and O_2 on Zr2E6 (pH 1.4).

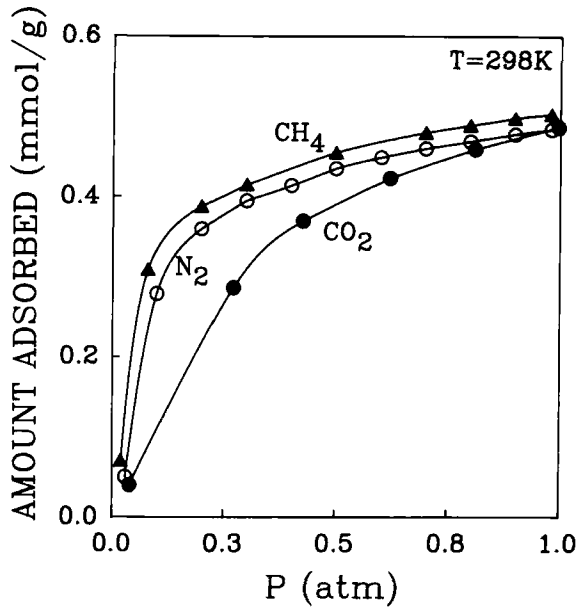

FIG. 3. Equilibrium isotherms of N_2, CH_4, and CO_2 on Zr2E6.

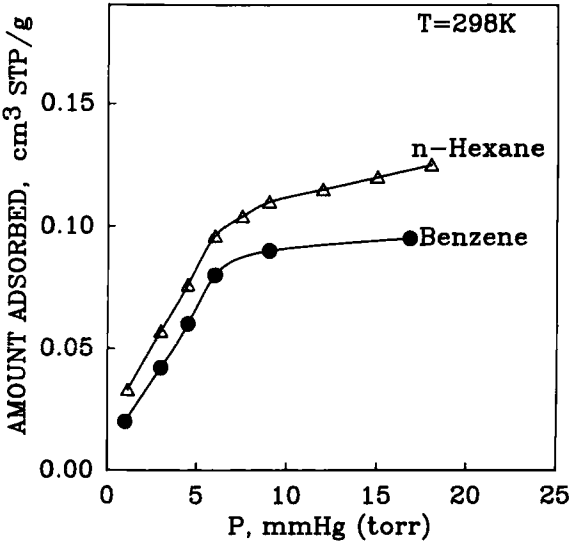

FIG. 4. Equilibrium isotherms of *n*-hexane and benzene on Zr2E6.

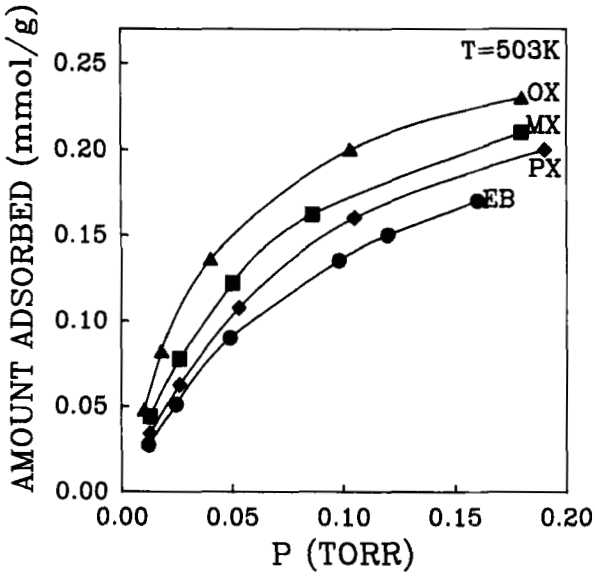

FIG. 5. Equilibrium isotherms of ethylbenzene (EB), *p*-xylene (PX), *m*-xylene (MX), and *o*-xylene (OX) on Zr2E6.

The adsorption isotherms of ethylbenzene (EB), *o*-xylene (OX), *m*-xylene (MX), and *p*-xylene (PX) at 503 K on Zr-pillared clay (Zr2E6) are displayed in Fig. 5. The isotherms at 503 K were selected for display, since this was the temperature that was used in the equilibrium separation of ethylbenzene/xylenes by gas chromatography. From the isotherms, ethylbenzene is the least strongly adsorbed, and *o*-xylene is the most strongly adsorbed. Thus, in equilibrium gas chromatographic separation, these compounds should elute the column in the order EB, PX, MX, OX as suggested by the relative equilibrium capacities.

Diffusivities

The uptake rates of O_2, N_2, CH_4, CO_2, hexane, benzene, ethylbenzene, and xylenes are displayed in Figs. 6–9. In Fig. 6 the relative uptake rates of O_2 and N_2 in Zr-PILC (Zr2E6) and Bergbau-Forschung carbon molecular sieves (CMS) are compared. Since O_2 has a smaller kinetic diameter than N_2 (3.46 compared to 3.64 Å), O_2 is expected to have a faster uptake rate than N_2. The faster diffusion of the adsorbates in Zr-pillared clay indicates that this CMS has smaller pore sizes than pillared clay. Figure 7 compares the uptake rates of CO_2, N_2, and CH_4 in Zr-pillared clay. The large dif-

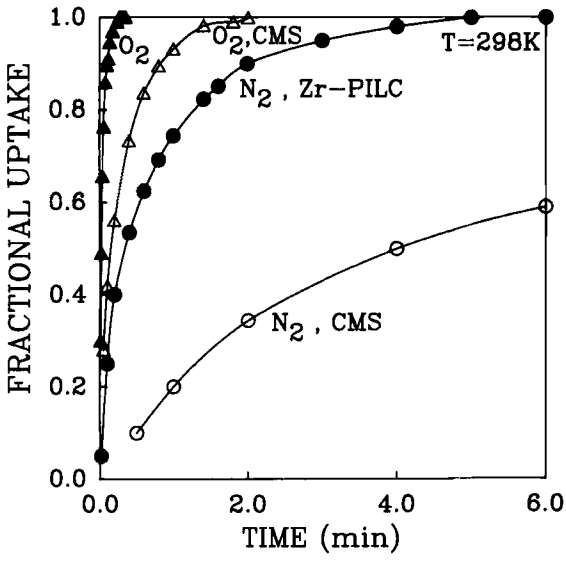

FIG. 6. Diffusion (uptake) rates of O_2 and N_2 in Zr-PILC (Zr2E6) compared with carbon molecular sieves (CMS).

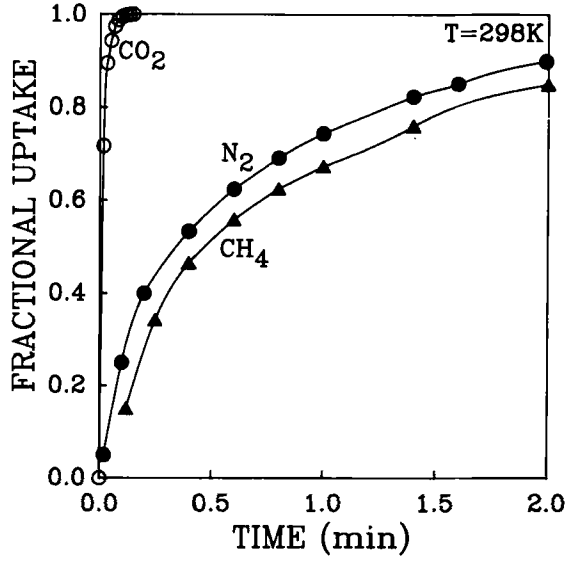

FIG. 7. Diffusion (uptake) rates of CO_2, N_2, and CH_4 in Zr2E6.

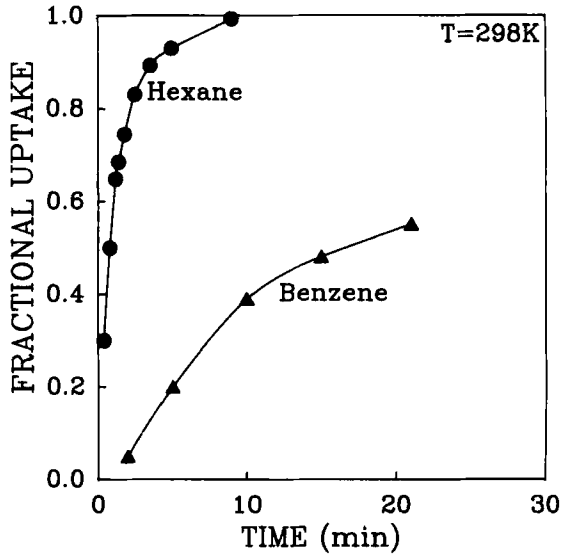

FIG. 8. Diffusion (uptake) rates of *n*-hexane and benzene in Zr2E6.

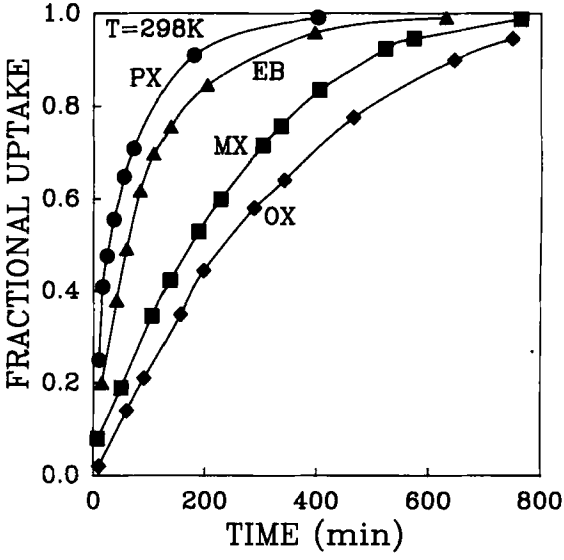

FIG. 9. Diffusion (uptake) rates of *p*-xylene (PX), ethylbenzene (EB), *m*-xylene (MX), and *o*-xylene (OX) in Zr2E6.

TABLE 1
Diffusion Time Constants for Various Adsorbates in Zr2E6 at 298 K

Adsorbate	Critical size (Å)	D/r_c^2 (s^{-1})
Carbon dioxide	3.3	15.3×10^{-2}
Oxygen	3.5	5.24×10^{-2}
Nitrogen	3.6	2.92×10^{-3}
Methane	3.8	2.16×10^{-3}
n-Hexane	4.9	1.73×10^{-3}
Benzene	6.7	6.20×10^{-5}
p-Xylene	6.7	2.02×10^{-5}
Ethylbenzene	6.6	4.12×10^{-6}
m-Xylene	7.4	2.73×10^{-6}
o-Xylene	7.4	2.37×10^{-6}
1,3,5-TMB	8.6	1.84×10^{-6}

ferences in the uptake rates of O_2 and N_2 (Fig. 6) or CO_2 and CH_4 (Fig. 7) indicate that kinetic separation of mixtures of these gases are possible. Indeed, we show in a later section that such separations can be accomplished using gas chromatography. Figures 8 and 9 show the uptake rates of various organic compounds on a zirconium pillared clay (Zr2E6), and the corresponding values of D_c/r_c^2 are listed in Table 1 for each of the adsorbates. It is obvious from Table 1 that the D_c/r_c^2 values for the adsorbates decrease with increasing adsorbate molecular size, and the largest adsorbate (1,3,5-TMB) has an extremely slow uptake rate.

X-Ray Diffraction Data

The x-ray diffraction patterns of three Zr-pillared clays and the bentonite clay have been shown elsewhere (*28*). The d_{001} peaks of the Zr-pillared clays occurred at lower 2θ values than that of the original clay. In all cases the d_{001} peaks of the Zr-pillared clays at 298 K were located at about $2\theta = 3.7°$, giving a d_{001} spacing of 23.85 Å. The free interlayer spacing was readily calculated by subtracting 9.6 Å (the thickness of the clay layer) from 23.85 Å, giving a free interlayer spacing of 14.3 Å.

Composition Analysis Using ICAP-AES

By using the ICAP-AES results of the bentonite clay listed in Table 2, a value of 103 mEq/100 g was obtained for the cation-exchange capacity (CEC). The CEC value was obtained by assuming that the only exchangeable cations of the bentonite clay were sodium, potassium, and calcium. From the results of Table 2, samples Zr2E6, Zr4E6, and Zr6E6 have 0.652,

TABLE 2
Chemical Compositions of a Bentonite Clay and Zr-Pillared Clays

Component (wt%)	Bentonite	Zr2E6	Zr4E6	Zr6E6
SiO_2	54.72	48.75	51.49	45.62
Al_2O_3	15.98	14.01	14.98	12.95
MgO	1.94	1.50	1.70	1.61
Fe_2O_3	2.93	2.49	2.78	2.44
TiO_2	0.12	0.12	0.19	0.12
Na_2O	2.04	0.22	0.39	1.39
CaO	0.82	0.09	0.40	0.72
ZrO_2	0.03	17.65	15.60	13.83
K_2O	0.34	0.27	0.23	0.26

0.552, and 0.547 Zr cations per formula unit. These values are lower than 0.698 which is required for a 100% exchange of the resident cations of the clay with Zr cations. The sample Zr2E6 was 93.4% exchanged, and the other two samples about 80% exchanged. These samples were prepared under identical conditions except for pH differences of the slurries during the synthesis.

Surface Area and Pore Volume of Zr-PILC

The surface areas and pore volumes of three pillared clays measured by various adsorbates and calculated by different methods have been described in detail (*28*). Only a summary is given here, shown in Table 3. The BET and Langmuir surface areas were both calculated from N_2 (77 K) adsorption data.

The N_2 pore volumes were measured by N_2 adsorption at 77 K, and the limiting pore volumes were calculated from the Dubinin-Astakhov equation.

Separations by Gas Chromatography

Based on the large difference in the uptake rates of CH_4 and CO_2 (Fig. 7), kinetic separation using a 50% mixture of CH_4 and CO_2 was investi-

TABLE 3
Physical Characterization of Zr-PILC: Surface Areas and Pore Volumes

Zr-PILC	BET (m^2/g)	Langmuir (m^2/g)	N_2 (cm^3/g)
Zr2E6	321.8	499.2	0.175
Zr4E6	195.7	371.9	0.120
Zr6E6	163.9	359.0	0.108

gated. The gas chromatogram for a 0.4-cm^3 pulse injection into a column containing Zr-pillared clay as the adsorbent is shown in Fig. 10 (bottom). Since CH_4 diffusion is much slower than CO_2 and the carrier gas flow rate relatively high (60 cm^3/min), methane was not allowed enough time to diffuse into the adsorbent. Thus, CH_4 eluted the column first, achieving a sharp kinetic separation of CH_4/CO_2. However, at lowest carrier gas flow rates, adequate diffusion time was allowed, and the separation was due to the difference in the affinity of the adsorbates on the adsorbent, an equilibrium separation results, leading to a complete reversal in the order of the elution peaks.

The feasibility of separating air by gas chromatography was also explored. To achieve kinetic separation of air, high carrier gas flow rate (above 60 cm^3/min) was required, while equilibrium separation required lower carrier gas flow rate ($\leq$10 cm^3/min). A 1/8 in. o.d. column containing

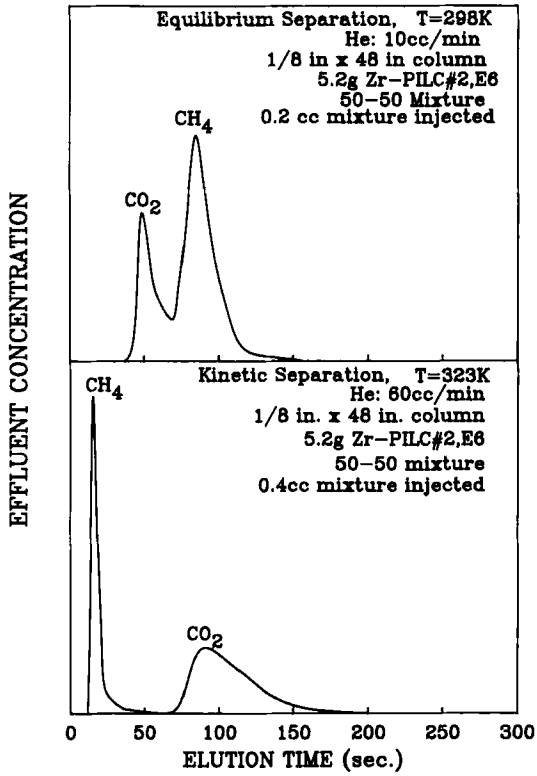

FIG. 10. Chromatographic separation of CH_4 and CO_2 by Zr2E6.

Zr-pillared clay was subjected to an inlet pressure of 15 psig for the equilibrium separation of air (see Fig. 11A), while a 1/4 in. o.d. column with an inlet pressure of 35 psig was used for the kinetic separation of air. At a flow rate of 30 cm^3/min through the 1/8 in. column, Fig. 11(B) shows that there was no separation. However, at 10 cm^3/min, Fig. 11(A) shows that separation was possible. Based on the adsorption isotherms of Fig. 2 and the chromatogram of Fig. 11(A), it is obvious that the separation was accomplished by equilibrium, since the isotherms of Fig. 2 indicate a N_2/O_2 selectivity. The chromatogram of Fig. 11(C) shows the kinetic separation of air. Such a separation was achieved using a 1/4 in. o.d. column having almost twice as much pillared clay, carrier gas flow rate of 60 cm^3/min, and an inlet pressure of 35 psig.

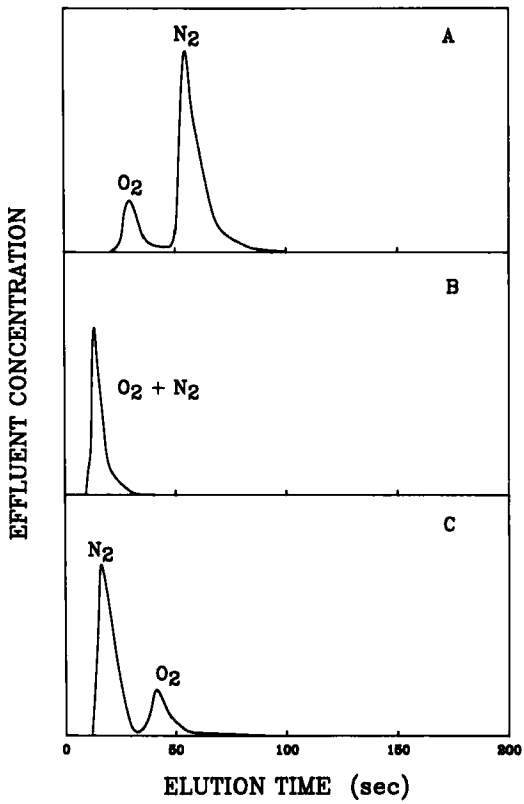

FIG. 11. Chromatographic separation of air at 298 K by Zr2E6. (A) Equilibrium separation with space velocity of 1.05 min^{-1}. (B) No separation with space velocity of 3.14 min^{-1}. (C) Kinetic separation with space velocity of 4.16 min^{-1}.

The separation of a 50/50 mixture of N_2 and CH_4 was accomplished in a 1/8 in. o.d. column. The chromatogram for this separation is shown in Fig. 12. It is obvious from this chromatogram (Fig. 12) and the adsorption isotherms (Fig. 3) that the separation is equilibrium, since the isotherms of Fig. 3 indicate CH_4 has a higher equilibrium selectivity than N_2.

The equilibrium adsorption isotherms of ethylbenzene (EB), *o*-xylene (OX), *m*-xylene (MX), and *p*-xylene (PX) at 503 K are displayed in Fig. 5. The chromatogram displayed in Fig. 13(A) shows that the components of a mixture (25% each) of ethylbenzene (EB) and xylenes (OX, MX, PX) are separated into four components and eluted the column in the order EB, PX, MX, and OX. Such elution sequence can be explained by using the adsorption isotherms for these components (Fig. 5). Based on the adsorption isotherms, *o*-xylene has the strongest affinity for the adsorbent and therefore is the last component to exit the column, while ethylbenzene has the least affinity for the adsorbent and is therefore the first component to elute the column.

By increasing the carrier gas flow rate to 75 cm^3, we were able to reverse the elution sequence of *o*-xylene and *p*-xylene, i.e., instead of having *p*-xylene eluting the column before *o*-xylene, which is required by the equilibrium isotherms (Fig. 5), *o*-xylene eluted the column before *p*-xylene. The results are displayed in Fig. 13(B). Since *p*-xylene diffuses faster than *o*-xylene in Zr-pillared clay, equilibrium separation was switched to kinetic separation by increasing the flow rate. However, since the diffusivities

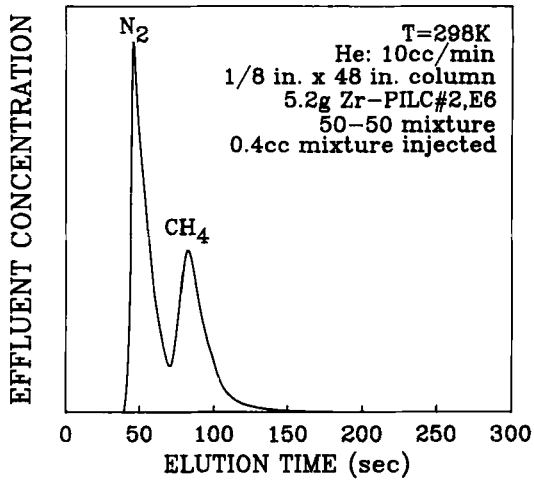

FIG. 12. Equilibrium chromatographic separation of N_2 and CH_4 at 298 K by Zr2E6.

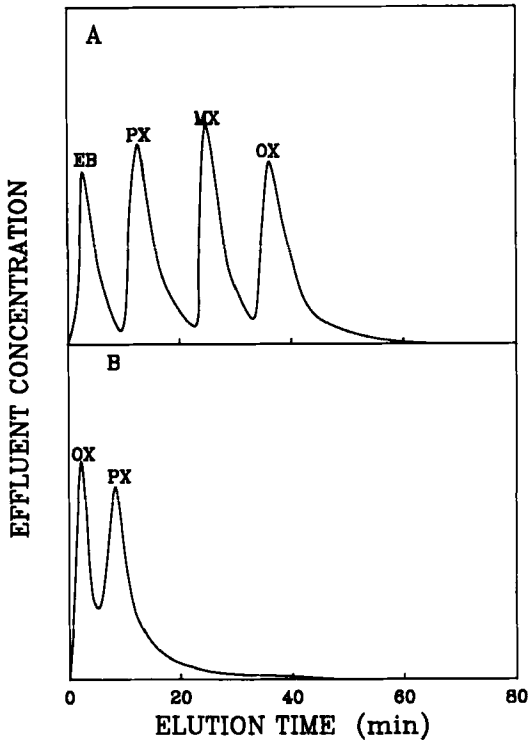

FIG. 13. Chromatographic separation of ethylbenzene (EB), *p*-xylene (PX), *m*-xylene (MX), and *o*-xylene (OX) by Zr2E6 at 503 K at the following space velocities: (A) 121.03 min^{-1} and (B) 105.9 min^{-1}.

of these isomers are not very different, we were unable to separate binary mixtures of ethylbenzene/*p*-xylene and *o*-xylene/*m*-xylene by kinetic separation. Nevertheless, it is possible to separate binary mixtures of ethylbenzene/*o*-xylene, ethylbenzene/*m*-xylene, *p*-xylene/*o*-xylene, and *p*-xylene/*m*-xylene by using a kinetic mode of operation and gas chromatography. Since the results for these binary mixtures are almost identical, only the binary mixture of *p*-xylene/*o*-xylene is shown (Fig. 13B).

The kinetic separation of mixtures of benzene and hexane using Zr-PILC is displayed in Fig. 14. Again, the high carrier gas flow rate and the differences in the diffusivities of the two components resulted in benzene (the slower diffusing species) and then hexane elutions in the order shown (Fig. 14).

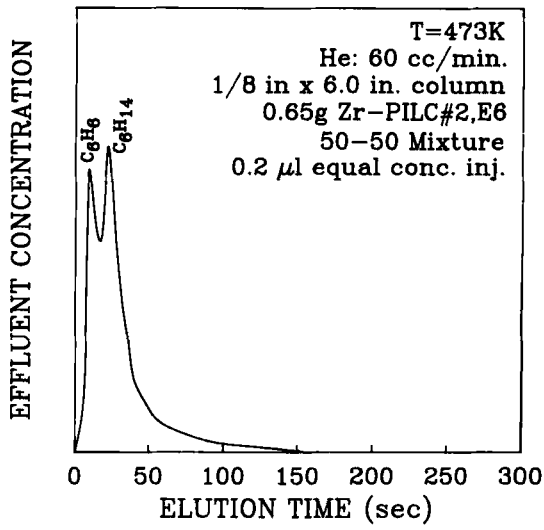

FIG. 14. Chromatographic separation of benzene (C_6H_6) and *n*-hexane (C_6H_{14}) at 473 K by Zr2E6.

Acknowledgment

This work was supported by the NSF under Grant CTS-8914754.

REFERENCES

1. G. W. Brindley and R. E. Sempels, *Clay Miner., 12,* 229 (1977).
2. N. Lahav, N. Shani, and J. Shabtai, *Clays Clay Miner., 26,* 107 (1978).
3. D. E. W. Vaughan, R. J. Lussier, and J. S. Magee, U.S. Patent 4,176,090 (1979).
4. R. H. Loeppart, M. M. Mortland, and T. J. Pinnavaia, *Clays Clay Miner., 27,* 201 (1979).
5. J. Shabtai, R. Lazar, and A. G. Oblad, in *Proc. 7th Int. Congr. Catal.* (T. Seiyama and K. Tanabe, eds.), Kodansha Elsevier, Tokyo, 1980, p. 828.
6. M. L. Occelli and R. M. Tindwa, *Clays Clay Miner., 31*(1), 22 (1983).
7. T. J. Pinnavaia, *Science, 220,* 365 (1983).
8. R. Burch (ed.), in *Catalysis Today,* Vol. 2, Elsevier, New York, 1988, p. 185.
9. F. Figueras, *Catal. Rev., Sci. Eng., 30*(3), 457 (1988).
10. C. F. Baes and R. E. Mesmer, *The Hydrolysis of Cations,* Wiley, New York, 1976.
11. A. Clearfield, in *NATO Adv. Study Inst. Ser., Ser. C, 231,* 271 (1988).
12. M. A. Drezdon, *Inorg. Chem., 27,* 4628 (1988).
13. R. Sprung, M. E. Davis, J. S. Kauffman, and C. Dybowski, *Ind. Eng. Chem. Res., 29,* 213 (1990).
14. M. L. Occelli, R. A. Innes, F. S. S. Hwu, and J. W. Hightower, *Appl. Catal., 14,* 69 (1985).
15. T. Bandosz, J. Jagiello, and M. Zyla, *Chem. Stosow., 33,* 189 (1989).
16. M. S. Tzou and T. J. Pinnavaia, in Ref. 8, p. 243.
17. S. Yamanaka and M. Hattori, in Ref. 8, p. 261.

18. M. Sahimi, T. T. Tsotsis, and M. L. Occelli, *Mater. Res. Soc. Symp. Proc., 111,* 271 (1988).
19. R. T. Yang, *Gas Separation by Adsorption Processes,* Butterworths, Boston, 1987.
20. H. S. Shin and K. S. Knaebel, *AIChE J., 34,* 1409 (1988).
21. Z. Pan, R. T. Yang, and J. A. Ritter, in *New Directions in Sorption Technology* (G. E. Keller Jr. and R. T. Yang, eds.), Butterworths, Boston, 1989.
22. A. Kapoor and R. T. Yang, *Chem. Eng. Sci., 44*(8), 1723 (1989).
23. M. W. Ackley and R. T. Yang, *AIChE J. 36,* 1229 (1990).
24. D. B. Broughton, R. W. Neuzil, J. M. Pharis, and C. S. Brearley, *Chem. Eng. Prog., 66*(9), 70 (1970).
25. S. Otani, *Chem. Eng., 80,* 106 (1973).
26. M. Seko, T. Miyake, and K. Inada, *Ind. Eng. Chem., Prod. Res. Dev., 18,* 263 (1979).
27. R. V. Jasra and S. G. T. Bhat, *Sep. Sci. Technol., 23*(10 & 11), 945 (1988).
28. R. T. Yang and M. S. A. Baksh, *AIChE J., 37,* 679 (1991).
29. Y. T. Yeh and R. T. Yang, *Ibid., 35,* 1659 (1989).
30. F. E. Lichte, D. W. Golightly, and P. J. Lamothe, in *Methods of Geochemical Analysis,* U.S. Geological Survey Bulletin 1770, United States Government Printing Office, Washington, D.C., 1987.

Received by editor November 8, 1990
Revised January 28, 1991